ResearchGate

See discussions, stats, and author profiles for this publication at: https://www.researchgate.net/publication/331943464

Electron redistribution and energy transfer in graphene/MoS 2 heterostructure

Article *in* Applied Physics Letters · March 2019

DOI: 10.1063/1.5088512

CITATION
1

READS
134

9 authors, including:

Weiyi Lin
Xiamen University
16 PUBLICATIONS **99** CITATIONS
SEE PROFILE

Harry Chou
University of Texas at Austin
37 PUBLICATIONS **2,961** CITATIONS
SEE PROFILE

Wei Li
University of Texas at Austin
98 PUBLICATIONS **864** CITATIONS
SEE PROFILE

Some of the authors of this publication are also working on these related projects:

Beyond Si CMOS View project

All content following this page was uploaded by Weiyi Lin on 20 October 2019.

The user has requested enhancement of the downloaded file.

Applied Physics Letters

Electron redistribution and energy transfer in graphene/MoS_2 heterostructure

Cite as: Appl. Phys. Lett. **114**, 113103 (2019); https://doi.org/10.1063/1.5088512
Submitted: 10 January 2019 . Accepted: 02 March 2019 . Published Online: 21 March 2019

Weiyi Lin, Pingping Zhuang, Harry Chou, Yuqian Gu, Richard Roberts, Wei Li, Sanjay K. Banerjee, Weiwei Cai, and Deji Akinwande

COLLECTIONS

This paper was selected as an Editor's Pick

View Online Export Citation CrossMark

Applied Physics Reviews
Now accepting original research
2017 Journal Impact Factor: 12.894

© 2019 Author(s).

Applied Physics Letters ARTICLE scitation.org/journal/apl

Electron redistribution and energy transfer in graphene/MoS_2 heterostructure

Cite as: Appl. Phys. Lett. **114**, 113103 (2019); doi: 10.1063/1.5088512
Submitted: 10 January 2019 · Accepted: 2 March 2019 ·
Published Online: 21 March 2019

View Online Export Citation CrossMark

Weiyi Lin,[1,2] Pingping Zhuang,[1,2] Harry Chou,[2,3] Yuqian Gu,[2] Richard Roberts,[2] Wei Li,[2] Sanjay K. Banerjee,[2] Weiwei Cai,[1,a)] and Deji Akinwande[2]

AFFILIATIONS

[1]Department of Physics, Xiamen University, Xiamen, Fujian 361005, China
[2]Department of Electrical and Computer Engineering, Microelectronic Research Center, The University of Texas at Austin, Austin, Texas 78758, USA
[3]Texas Materials Institute, The University of Texas at Austin, Austin, Texas 78712, USA

[a)]Author to whom correspondence should be addressed: wwcai@xmu.edu.cn

ABSTRACT

In this letter, van der Waals heterostructures (vdWHs) assembled by molybdenum disulfide (MoS_2) and graphene monolayers are used as an experimental prototype to study the interaction between two-dimensional (2D) semiconducting and semimetal materials. The electron redistribution and energy transfer in graphene/MoS_2 vdWHs are demonstrated by the combination of electrical measurements (Dirac-point shift) and Raman analyses. In graphene, the linear dispersive Dirac fermions can resonate with various-frequency "photons," which "emit" from optically active MoS_2 by the recombination of in-plane excitons. The experimental finding suggests that the photon-induced charge separation and accumulation might be in a low degree, thus affecting the performance of semiconductor/graphene-based 2D optoelectronic devices.

Published under license by AIP Publishing. https://doi.org/10.1063/1.5088512

In two-dimensional van der Waals heterostructures (vdWHs), wave-function overlaps between stacked layers serve as electron-exchange paths, which contribute to the electron redistribution.[1] Nonequilibrium charge carriers excited by photon impingements in different materials can transfer through vdW interfaces in an energetically favorable manner, prior to the recombination of electron-hole pairs.[2,3] This charge transfer process accompanied by non-radiative vibrational relaxations is capable of reducing the amount of emitting photons in optically active materials.[4] Additionally, because the separation distance between stacked layers in vdWHs could be as small as several Å, energy transfer including (i) concerted tunneling of charge carriers[5] (Dexter type) and (ii) dipole-dipole interaction[6] (Förster type) is allowed to occur at the interface. This is also a well-known underlying mechanism governing quenching phenomena in photoluminescence (PL) and fluorescence. For instance, in graphene/transition metal dichalcogenide (TMD) vdWHs, PL quenching of TMDs materials was observed and both charge- and energy-transfer processes were demonstrated by various optical spectroscopy techniques.[7,8] These optical phenomena can be partially attributed to the electronic delocalization and semi-metal properties of graphene.

Recent optical spectroscopy analyses have demonstrated that energy transfer governs PL quenching in graphene/molybdenum diselenide ($MoSe_2$) vdWHs,[9] in which the Dirac point of graphene lies near the median position of the band gap of $MoSe_2$, whose electron and hole effective masses are very close.[10] However, in the case of graphene/molybdenum disulfide (MoS_2) vdWHs, the PL quenching has been regarded to be primarily attributed to the photo-induced charge transfer.[11] The Dirac point of graphene lies close to the conduction band edge of MoS_2 (Ref. 12). Compared with the band offset of graphene/$MoSe_2$, the one of graphene/MoS_2 is more favorable for the interlayer charge transfer.[13,14] In fact, the large in-plane excitons in MoS_2 (Ref. 15) should favor Förster resonance energy transfer to graphene, in which the linear dispersive Dirac fermions can resonate with various-frequency photons.[16] Nevertheless, a debate on the relative importance of the two transfer processes remains. Here, we use graphene/MoS_2 vdWHs as an experimental prototype to study the interaction between TMDs and graphene.

Graphene, MoS_2, and multilayer hexagonal boron nitride (hBN) are synthesized by chemical vapor deposition (CVD) methods[17–19] (S1–S4 in the supplementary material). Then, graphene and hBN (capping layer) are transferred onto MoS_2/SiO_2 substrates using PMMA-based techniques to obtain vdWHs [Fig. 1(a)]. From the optical image, we can clearly discern hBN-covered triangular MoS_2 domains, graphene, and graphene/MoS_2 regions [Fig. 1(b); for Raman

Published under license by AIP Publishing

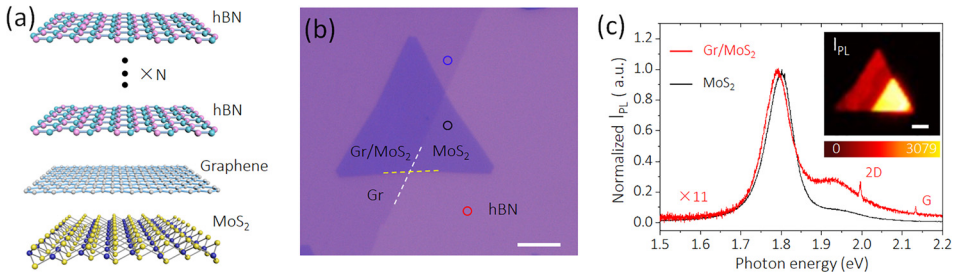

FIG. 1. (a) An illustration of the vdWH assembled from monolayer MoS_2, monolayer graphene, and multilayer hBN. (b) Optical image of the vdWH. Gr denotes graphene. (c) PL spectra of MoS_2 (black) and graphene/MoS_2 vdWH (red) obtained by using low Φ_{ph} ($\sim 1 \times 10^{23}$ cm^{-2} s^{-1}). Φ_{ph} can be estimated by $\Phi_{ph} = \pi P N_A{}^2/\hbar\omega_i\lambda^2$, where P denotes the laser power, N_A the numerical aperture (0.75 for the ×50 working-distance objective used here), $\hbar\omega_i$ the incident photon energy, and λ the wavelength. The inset is the PL-intensity map of the vdWH. The red curve shows two peaks corresponding to graphene Raman modes 2D (~332 meV) and G (~196 meV). The excitation energy is 2.33 eV. Scale bar = 5 μm.

maps and spectra, see S5 and S6 in the supplementary material]. The following discussion is based on the existence of the hBN capping layer except where otherwise noted. As shown in Fig. 1(c), the PL intensity of MoS_2 is quenched by graphene by ~1 order of magnitude. In the graphene/MoS_2 PL spectrum, two sharp peaks are located at ~1.99 and ~2.13 eV, which correspond to Raman-shift energies of ω_{2D} and ω_G, respectively, confirming the role of the graphene layer (S7 in the supplementary material). In addition to the main peak, there is a shoulder with higher energy owing to spin-orbit interaction induced band splitting of the valence band in MoS_2 (Refs. 20 and 21) Generally, most of the monolayer MoS_2 belongs to n-type such that holes occupy electronic states of the higher-energy splitting branch in the valence band.[22,23] Therefore, in this study, we focus on the high-intensity low-energy excitonic peak. In the following, we discuss the governing mechanism by analyzing electrical measurements and Raman spectra of graphene/MoS_2 vdWHs.

With the aid of interlayer wave-function overlaps, charge carriers may travel through the interface to reduce the Fermi-level difference between stacked layers. This process can be determined by measuring the Dirac point (V_{Dirac}) shift of graphene-embedded field effect transistors [FETs; Figs. 2(a) and 2(b)]. For all FETs, source and drain electrodes come in contact with graphene [Fig. 2(c)]. By changing the back-gate bias (V_g), we tune the source-drain resistance (R_{sd}) as shown in Figs. 2(d) and 2(e). V_{Dirac} of both graphene and graphene/MoS_2 having hBN capping layers is red-shifted relative to the value of uncovered samples. Compared with V_{Dirac} of MoS_2-absent graphene samples, the value of graphene/MoS_2 is also red-shifted in both with and without hBN cases. In thermal equilibrium under zero gate voltage, the Fermi level (E_F) can be estimated as

$$E_F - E_{Dirac} = \pm\sqrt{\pi C_i |q|^{-1}}\hbar\nu_F \cdot \sqrt{|V_{Dirac}|}, \quad (1)$$

where q denotes the charge of carriers; $\hbar$ the reduced Planck constant; ν_F ($\sim 10^6$ m/s) the Fermi velocity of graphene; $C_i = \varepsilon_0\varepsilon_r(d)^{-1}$ the capacitance; and $E_{Dirac} = 0$ for convenience.[2] Accordingly, the existence of hBN films elevates graphene's Fermi level (−267 to −188 meV for graphene; −209 to −140 meV for graphene/MoS_2), indicating that the insulating capping layer reduces p-type doping effects. Importantly, the Fermi level of graphene/MoS_2 is higher than the one of MoS_2-absent graphene samples, suggesting that the hole concentration in graphene decreases in vdWHs. However, unlike graphene/fluorescent molecule systems we reported previously, in which V_{Dirac} of graphene is altered by the charge transfer under visible-light impingements,[2] V_{Dirac} of graphene/MoS_2 behaves light-independent. This observation suggests that (i) electrons redistribute in graphene/MoS_2 vdWHs and (ii) most of the photon-excited electron-hole pairs in MoS_2 may not be separated spatially. Note that depletion regions in van der Waals interfaces could be absent, and it is difficult to illustrate whether the Fermi level in graphene and MoS_2 do equilibrate or not.

The variation of the charge-carrier concentration can also be determined by measuring the ω shift for Raman-active phonon modes that are strongly coupled with electrons. For instance, ω_G of graphene is sensitive to doping because of the non-adiabatic electron-phonon

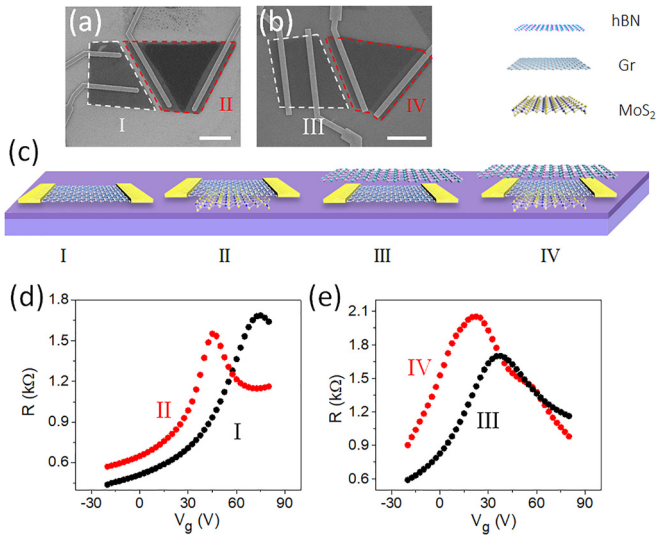

FIG. 2. (a) and (b) SEM images of FETs. These transistors consist of SiO_2 (285 nm)/Si substrates, Ti (2 nm)/Au (45 nm) electrodes, and conducting channels including graphene (I), graphene/MoS_2 (II), hBN/graphene (III), and hBN/graphene/MoS_2 (IV). Ti/Au electrodes are deposited on graphene layers. Scale bar = 5 μm. (c) Schematic of FETs. (d) and (e) The $R_{sd} - V_g$ measurements of FETs without and with the hBN capping layer. V_{sd} = 100 mV. The Dirac point locates at 73 V, 45 V, 36 V, and 20 V, respectively.

Published under license by AIP Publishing

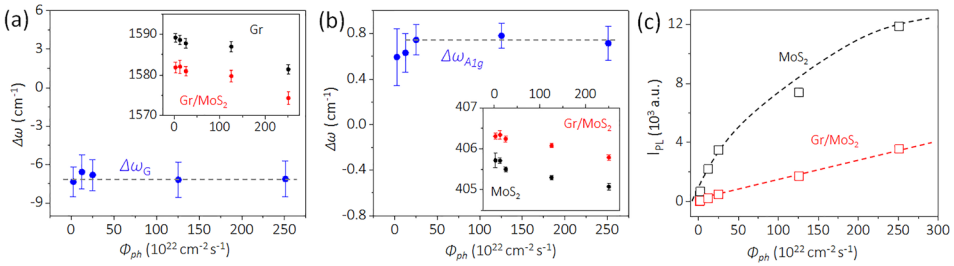

FIG. 3. (a) The scatter plot of $\Delta\omega_G$ versus incident Φ_{ph}. $\Delta\omega_G = \omega_G$ (graphene/MoS_2) $- \omega_G$(graphene). The inset is the scatter plot of the ω_G for graphene (black) and graphene/MoS_2 (red) versus incident Φ_{ph}. (b) The scatter plot of $\Delta\omega_{A_{1g}}$ versus incident Φ_{ph}. $\Delta\omega_{A_{1g}} = \omega_{A_{1g}}$ (graphene/MoS_2) $- \omega_{A_{1g}}$ (MoS_2); The inset is the scatter plot of the $\omega_{A_{1g}}$ for MoS_2 (black) and graphene/MoS_2 (red) versus incident Φ_{ph}. (c) The scatter plot of I_{PL} versus Φ_{ph} for MoS_2 (black) and graphene/MoS_2 (red) regions. Dashed lines are guides to the eye.

coupling,[24,25] which results in ω_G softening under the reduction of $|\Delta E|$ ($|\Delta E| = \left|E_F^{Gr} - E_{Dirac}\right|$, where E_{Dirac} denotes the energy value at the Dirac cone vertex). Generally, CVD-grown graphene that is transferred onto a SiO_2 substrate is p-type doped due to the absorption of molecules with relatively large electron affinity.[26] We observe that ω_G of graphene/MoS_2 vdWH is red-shifted with respect to that of MoS_2-absent graphene, thus suggesting that the hole-concentration decreases in graphene and the Fermi surface moves toward E_{Dirac} (S8 in the supplementary material). For the case of MoS_2, $\omega_{A_{1g}}$ is monotonically blue-shifted with the decrease in electron concentration owing to doping-induced phonon renormalization.[27] A blueshift behavior ($\sim$0.8 cm^{-1}) of $\omega_{A_{1g}}$ further confirms that electrons in MoS_2 transfer to graphene (S9 in the supplementary material). This peak-position variation based on Raman analyses is in agreement with electrical measurements shown in Fig. 2.

As Φ_{ph} increases, ω_G of both MoS_2-absent graphene and graphene/MoS_2 is red-shifted because of the laser-induced heating. The difference of ω_G between graphene and graphene/MoS_2 approaches saturation values as Φ_{ph} is increased [Figs. 3(a) and S10–S12 in the supplementary material]. Similarly, the difference of $\omega_{A_{1g}}$ between MoS_2 and graphene/MoS_2 approaches saturation values as Φ_{ph} is increased [Figs. 3(b), S13, and S14 in the supplementary material]. Remarkably, the I_{PL}/Φ_{ph} ratio of MoS_2 drops as Φ_{ph} is increased (S15 in the supplementary material), whereas I_{PL} of graphene/MoS_2 increases linearly with Φ_{ph} of up to 10^{24} cm^{-2} s^{-1} [Fig. 3(c)]. Similar quenching behavior is also observed by using 442 nm-wavelength laser light (S16 in the supplementary material).

These observations based on Raman analyses and electrical measurements indicate that (a) electrons redistribute in vdWHs with respect to separated materials and (b) increasing Φ_{ph} will not further transfer net charges once the system reaches a saturation value. In the saturation regime, no net charge transfer occurs, whereas the quenching efficiency persists. The accumulation of large amounts of photon-generated excitons in MoS_2, which is a strongly confined two-dimensional system, gives rise to efficient exciton-exciton annihilation (EEA)[28,29] at high Φ_{ph}, leading to the reduction of the I_{PL}/Φ_{ph} ratio. In contrast, because graphene's Fermi level lies between the conduction- and valence-band edges of MoS_2, photo-generated electrons and holes in the MoS_2 are allowed to transfer to graphene as long as energy and momentum are conserved. Additionally, the linear dispersion of Dirac fermions allows electron-hole pairs in graphene to resonate with various-frequency virtual photons[16] that "emit" from MoS_2. On the one hand, such energy transfer processes between graphene and MoS_2 greatly reduce exciton lifetime, and thus, the EEA effect in graphene/MoS_2 is suppressed. On the other hand, energy transfer in graphene/MoS_2 vdWHs is capable of providing highly efficient relaxation paths for excitons, quenching the PL intensity massively, and thus leading to the linear rise of PL intensity with Φ_{ph} even the system is under the saturation regime that no net charge transfer occurs.

In summary, graphene/MoS_2 vdWHs are fabricated and characterized. We find that the PL intensity of MoS_2 is significantly quenched by the existence of graphene and rises linearly with Φ_{ph}. Based on the Dirac point shift of graphene, we conclude that electrons redistribute in vdWHs with respect to separated graphene and MoS_2. As incident Φ_{ph} increases, the Fermi level of graphene moves to a saturation value evidenced by Raman analyses. In the saturation regime, where not net charge transfer occurs, the PL quenching efficiency remains unchanged. These analyses suggest that the quenching phenomenon observed in graphene/MoS_2 is dominantly governed by energy transfer. However, in graphene/TMD vdWH systems, both Dexter type energy transfer and Förster type energy transfer are expected to occur, and techniques employed in this study are not able to unambiguously distinguish the two types of energy transfer. Additionally, conducting *in-situ* low-temperature Raman and PL measurements on vdWHs under various back-gate biases should provide a more comprehensive understanding of excitonic dynamics and transfer processes in graphene-TMD vdWHs.

See supplementary material for Methods: (1) materials syntheses, (2) characterizations, and (3) device fabrication and measurements and Figs. S1–S16.

This work was supported by the National Natural Science Foundation of China (Grant No. 11335006), Fok Ying Tung Education Foundation, and the U.S. Army Research Office under MURI Award No. W911NF-17-1-0312. We acknowledge the use of Texas Nanofabrication Facilities supported by the NSF NNCI Award No. 1542159. We also acknowledge the China Scholarship Council (CSC) scholarship under the State Scholarship Fund. D. A acknowledges the support of the PECASE award from the army research office.

REFERENCES

[1]H. Wang, J. Bang, Y. Y. Sun, L. B. Liang, D. West, V. Meunier, and S. B. Zhang, Nat. Commun. 7, 11504 (2016).

Published under license by AIP Publishing

[2]W. Y. Lin, B. Tian, P. P. Zhuang, J. Yin, C. K. Zhang, Q. Y. Li, T. M. Shih, and W. W. Cai, Nano Lett. **16**(9), 5737–5741 (2016).
[3]H. Xu, X. Y. Han, X. Dai, W. Liu, J. Wu, J. T. Zhu, D. Y. Kim, G. F. Zou, K. A. Sablon, A. Sergeev, Z. X. Guo, and H. Y. Liu, Adv. Mater. **30**(13), 1706561 (2018).
[4]H. S. S. R. Matte, K. S. Subrahmanyam, K. V. Rao, S. J. George, and C. N. R. Rao, Chem. Phys. Lett. **506**(4-6), 260–264 (2011).
[5]D. L. Dexter, J. Chem. Phys. **21**(5), 836–850 (1953).
[6]D. Kozawa, A. Carvalho, I. Verzhbitskiy, F. Giustiniano, Y. Miyauchi, S. Mouri, A. H. C. Neto, K. Matsuda, and G. Eda, Nano Lett. **16**(7), 4087–4093 (2016).
[7]L. Yuan, T. F. Chung, A. Kuc, Y. Wan, Y. Xu, Y. P. Chen, T. Heine, and L. B. Huang, Sci. Adv. **4**(2), e1700324 (2018).
[8]J. Q. He, N. Kumar, M. Z. Bellus, H. Y. Chiu, D. W. He, Y. S. Wang, and H. Zhao, Nat. Commun. **5**, 5622 (2014).
[9]G. Froehlicher, E. Lorchat, and S. Berciaud, Phys. Rev. X **8**, 011007 (2018).
[10]A. Kormanyos, G. Burkard, M. Gmitra, J. Fabian, V. Zolyomi, N. D. Drummond, and V. Fal'ko, 2D Mater. **2**, 022001 (2015).
[11]H. Ago, H. Endo, P. Solis-Fernandez, R. Takizawa, Y. Ohta, Y. Fujita, K. Yamamoto, and M. Tsuji, ACS Appl. Mater. Interfaces **7**(9), 5265–5273 (2015).
[12]J. Kang, S. Tongay, J. Zhou, J. B. Li, and J. Q. Wu, Appl. Phys. Lett. **102**, 012111 (2013).
[13]H. Xu, J. X. Wu, Q. L. Feng, N. N. Mao, C. M. Wang, and J. Zhang, Small **10**(11), 2300–2306 (2014).
[14]W. J. Zhang, C. P. Chuu, J. K. Huang, C. H. Chen, M. L. Tsai, Y. H. Chang, C. T. Liang, Y. Z. Chen, Y. L. Chueh, J. H. He, M. Y. Chou, and L. Li, J. Sci. Rep.-UK **4**, 3826 (2014).
[15]J. A. Schuller, S. Karaveli, T. Schiros, K. L. He, S. Y. Yang, I. Kymissis, J. Shan, and R. Zia, Nat. Nanotechnol. **8**(4), 271–276 (2013).
[16]F. Bonaccorso, Z. Sun, T. Hasan, and A. C. Ferrari, Nat. Photonics **4**(9), 611–622 (2010).
[17]X. S. Li, W. W. Cai, J. H. An, S. Kim, J. Nah, D. X. Yang, R. Piner, A. Velamakanni, I. Jung, E. Tutuc, S. K. Banerjee, L. Colombo, and R. S. Ruoff, Science **324**(5932), 1312–1314 (2009).
[18]J. Zhang, H. Yu, W. Chen, X. Z. Tian, D. H. Liu, M. Cheng, G. B. Xie, W. Yang, R. Yang, X. D. Bai, D. X. Shi, and G. Y. Zhang, ACS Nano **8**(6), 6024–6030 (2014).
[19]P. P. Zhuang, W. Y. Lin, B. B. Xu, and W. W. Cai, Appl. Phys. Lett. **111**, 203103 (2017).
[20]K. F. Mak, K. L. He, J. Shan, and T. F. Heinz, Nat. Nanotechnol. **7**(8), 494–498 (2012).
[21]K. F. Mak, C. Lee, J. Hone, J. Shan, and T. F. Heinz, Phys. Rev. Lett. **105**, 136805 (2010).
[22]N. Scheuschner, O. Ochedowski, A. M. Kaulitz, R. Gillen, M. Schleberger, and J. Maultzsch, Phys. Rev. B **89**, 125406 (2014).
[23]B. Radisavljevic, A. Radenovic, J. Brivio, V. Giacometti, and A. Kis, Nat. Nanotechnol. **6**(3), 147–150 (2011).
[24]M. Lazzeri and F. Mauri, Phys. Rev. Lett. **97**, 266407 (2006).
[25]S. Pisana, M. Lazzeri, C. Casiraghi, K. S. Novoselov, A. K. Geim, A. C. Ferrari, and F. Mauri, Nat. Mater. **6**(3), 198–201 (2007).
[26]O. Leenaerts, B. Partoens, and F. M. Peeters, Phys. Rev. B **77**, 125416 (2008).
[27]B. Chakraborty, A. Bera, D. V. S. Muthu, S. Bhowmick, U. V. Waghmare, and A. K. Sood, Phys. Rev. B **85**, 161403(R) (2012).
[28]D. Z. Sun, Y. Rao, G. A. Reider, G. G. Chen, Y. M. You, L. Brezin, A. R. Harutyunyan, and T. F. Heinz, Nano Lett. **14**(10), 5625–5629 (2014).
[29]N. Kumar, Q. N. Cui, F. Ceballos, D. W. He, Y. S. Wang, and H. Zhao, Phys. Rev. B **89**(12), 125427 (2014).

Published under license by AIP Publishing

View publication stats